

## ON THE ROLE OF SECONDARY INTERACTIONS IN PRODUCTION OF BREMSSTRAHLUNG SPECTRA FROM A THICK TARGET

*Nguyen Tuan Khai<sup>a</sup>, Tran Duc Thiep<sup>a</sup>, Truong Thi An<sup>a</sup>, Phan Viet Cuong<sup>a</sup>,  
Nguyen The Vinh<sup>a</sup>, A. G. Belov<sup>b</sup>, O. D. Maslov<sup>b</sup>*

<sup>a</sup> Institute of Physics and Electronics, Hanoi, Vietnam

<sup>b</sup> Joint Institute for Nuclear Research, Dubna

Bremsstrahlung emission, or radiation loss, is a dominant mechanism for energy dissipation of electron at relativistic energies greater than a few MeV when it is subjected to acceleration in the field of the nucleus or of the electrons. In this work the Monte-Carlo calculations for bremsstrahlung spectra have been described for the case of thick tungsten target at the incident electron beams from 10 to 50 MeV, where secondary interactions induced by the electrons and photons in the target such as energy loss, absorption, scattering and  $(e^+, e^-)$ -pair production effects were taken into account.

В настоящей работе проведены вычисления спектров тормозного излучения из толстой вольфрамовой мишени с помощью метода Монте-Карло с учетом вторичных взаимодействий электронов и фотонов с мишенью для энергий электронов 10–50 МэВ.

PACS: 78.70.Ck

### INTRODUCTION

The bremsstrahlung emissions produced from accelerators are intensive and high-energy photon sources. They are widely used in photonuclear reaction research and applied nuclear physics. For example, to obtain the dependence of the cross sections of the photonuclear reactions on the photon energy, it is necessary to know the bremsstrahlung spectrum as a function of the incident electron energy. As there is not enough experimental data available, improvements in calculation technique based on updating the data of electron and photon are proved to be a good resolution for bremsstrahlung spectral evaluation for the above-mentioned goals of research.

The bremsstrahlung emissions have been calculated by several semi-analytical methods [1, 2]. However, due to difficulties in describing analytically the secondary interaction effects that occur in the target, especially those related to nonzero observation angles, these calculations are limited when a thick target is used, where the effect of secondary interactions cannot be ignored.

In this work we would like to use Monte-Carlo calculations based on the experimental data and theory about energy and angular distributions to consider the role of the secondary interaction processes induced by electrons and photons in thick tungsten target. This is necessary in evaluating accurately the production yield and spectral intensity corresponding to an incident electron beam.

### 1. CALCULATION TECHNIQUE

In principle, bremsstrahlung can be emitted whenever a charged particle experiences a change in its velocity under the influence of the Coulomb field of a nucleus. Since the rate of energy dissipation due to bremsstrahlung and the cross section for its production are inversely proportional to the square of the mass of the incident particle [4]:

$$\frac{dE_b}{dt} \sim \frac{Z^2 Z_t^2}{m^2}, \quad (1)$$

$$\sigma_b \sim Z_t^2 \left( \frac{e^2}{mc^2} \right)^2, \quad (2)$$

where  $m$  and  $Z$  are, respectively, the mass and the charge of the particle, and  $Z_t$  is the atomic number of the target. Bremsstrahlung emission is a dominant energy dissipation mechanism for electron, the lightest charge particle, especially at relativistic energies greater than a few MeV.

The study on angular distribution of bremsstrahlung [4–6] indicated that at very low energies of electrons the radiation intensity is of maximum in a direction perpendicular to the incident beam. However, as the energy is increased, the maximum appears at increasingly forward angles and in the limit of very high electron energies, the emission of bremsstrahlung essentially occurs as a narrow pencil in the forward direction. The average angle of emission is then given by [6]

$$\theta_\gamma \approx \frac{m_e c^2}{E_e}, \quad (3)$$

with  $E_e$  being the total energy of the incident electron;  $m_e c^2$  is the rest energy of electron.

Simulation for production of the bremsstrahlung and scattered electrons when a relativistic incident electron beam hits the thick target has been mentioned in the previous research [3]. In this work we concentrate on considering the role of the secondary processes that occur in the target due to the appearance of these particles in the formation of the final bremsstrahlung spectrum. The consideration can be summarized as follows:

1. Due to the bremsstrahlung emission under the influence of the Coulomb field of the nucleus, the incident electron will lose an amount of energy that is equal to the bremsstrahlung energy emitted (because  $M_{\text{nucl}} \gg m_e$ , the recoil energy of the nucleus can be ignored) and will be deflected from its moving direction. The remaining energy ( $T_s$ ) and reflection angle ( $\theta_e$ ) of the electron can be, therefore, determined using laws of conservation of energy and momentum as follows:

$$T_s = T_e - h\nu, \quad (4)$$

$$\gamma_s m_e v_s \cos(\theta_e) + \frac{h \cos(\theta_\gamma)}{\lambda} = \gamma_e m_e v_e, \quad (5)$$

where  $\theta_\gamma$  is given by formula (3);  $\beta$  and  $\gamma$  are the Lorentz factors of the electron;  $v_e$  and  $v_s$  are velocities of the incident and scattered electrons.

2. Since the bremsstrahlung production yield is proportional to the strength of the nuclear Coulomb field felt by the electron and the number of its interaction with the nuclei in the target, the intensity of its emission increases with atomic number and thickness of the braking target. However, bremsstrahlung radiation intensity can be considerably reduced by the attenuation

effects in the heavy target material. The data on photon cross sections for a given material in a wide range of energies from 100 keV to 100 MeV are parameterized as a function of the photon energy [7]:

$$\ln(\sigma_a) = a_0 + a_1 \ln(E) + a_2 \ln^2(E) + a_3 \ln^3(E), \quad (6)$$

$$\ln(\sigma_s) = b_0 + b_1 \ln(E) + b_2 \ln^2(E) + b_3 \ln^3(E), \quad (7)$$

$$\ln(\sigma_p) = c_0 + c_1 \ln(E) + c_2 \ln^2(E) + c_3 \ln^3(E), \quad (8)$$

where  $(a_0, a_1, a_2, a_3)$ ,  $(b_0, b_1, b_2, b_3)$  and  $(c_0, c_1, c_2, c_3)$  are fitting coefficients for the cross sections of photoelectric absorption, scattering and pair production processes, respectively.

a) For the photoelectric effect a quantum can be absorbed if  $E_\gamma > B_{\text{shell}}$ , where  $B_{\text{shell}}$  are the shell energies of electron. The photoelectron is emitted with kinetic energy:

$$T_{\text{pe}} = E_\gamma - B_{\text{shell}}. \quad (9)$$

The polar angle of the photoelectron is determined from the Sauter–Gavrila distribution for  $K$  shell [8]:

$$\cos \theta_{\text{pe}} = \frac{(1 - 2\gamma) + \beta}{(1 - 2\gamma)\beta + 1}, \quad (10)$$

where  $\beta$  and  $\gamma$  are the Lorentz factors of the photoelectron.

b) For the Compton scattering process the energy and angle of the scattered photon are determined as follows: Starting from the quantum mechanical Klein–Nishina differential cross section for Compton scattering [9]

$$\frac{d\sigma}{d\varepsilon} = \pi r_e^2 \left( \frac{m_e c^2}{E_0} \right) Z \left( \frac{1}{\varepsilon + \varepsilon} \right) \left[ 1 - \frac{\varepsilon \sin^2 \theta_{\text{Compt}}}{1 + \varepsilon^2} \right], \quad (11)$$

where  $r_e$  is the classical electron radius;  $m_e c^2$  is the electron mass;  $E_0$  is the energy of the incident photon;  $E_1$  is the energy of the scattered photon and  $\varepsilon = E_1/E_0$ .

Assuming an elastic collision, the scattering angle  $\theta_{\text{Compt}}$  is given by the Compton formula

$$E_1 = \frac{E_0 m_e c^2}{m_e c^2 + E_0 (1 - \cos \theta_{\text{Compt}})}. \quad (12)$$

The energy of scattered photons is sampled as follows:

The value of  $\varepsilon$  corresponding to the minimum photon energy, i.e., to backward scattering  $\theta_{\text{Compt}} = 180^\circ$ , is

$$\varepsilon_0 = \frac{m_e c^2}{m_e c^2 + 2E_0}. \quad (13)$$

Hence  $\varepsilon \in [\varepsilon_0, 1]$ . Using the combined composition and rejection Monte-Carlo method described in [9], we set a function depending on  $\varepsilon$  from the expression of the differential cross section:

$$\Phi(\varepsilon) = \left( \frac{1}{\varepsilon} + \varepsilon \right) \left[ 1 - \frac{\varepsilon \sin^2 \theta_{\text{Compt}}}{1 + \varepsilon^2} \right] = f(\varepsilon)g(\varepsilon), \quad (14)$$

$$= [\alpha_1 f_1(\varepsilon) + \alpha_2 f_2(\varepsilon)]g(\varepsilon), \quad (15)$$

where  $\alpha_1 = \ln(1/\varepsilon_0)$ ;  $f_1(\varepsilon) = 1/\alpha_1\varepsilon$ ;  $\alpha_2 = (1 - \varepsilon_0^2)/2$ ;  $f_2(\varepsilon) = \varepsilon/\alpha_2$ ;  $f_1$  and  $f_2$  are probability density functions defined on the interval  $[\varepsilon_0, 1]$ ;  $g(\varepsilon) = [1 - \varepsilon \sin^2 \theta_{\text{Compt}}/(1 + \varepsilon^2)]$  is the rejection function with all the values of  $\varepsilon$  to be taken in the interval  $[\varepsilon_0, 1]$ , so  $0 < g(\varepsilon) \leq 1$ .

Then the sampling procedure for  $\varepsilon$  can be summarized as follows:

- (i) generate a set of three random numbers  $q_1, q_2, q_3$  uniformly distributed on the interval  $[0, 1]$ ;
- (ii) decide where to sample from  $f_1(\varepsilon)$  or  $f_2(\varepsilon)$ : if  $q_1 < \alpha_1/(\alpha_1 + \alpha_2)$  select  $f_1(\varepsilon)$ , otherwise select  $f_2(\varepsilon)$ ;
- (iii) sample  $\varepsilon$  from the distributions corresponding to  $f_1$  or  $f_2$ :  
 $\varepsilon = \exp(-q_2\alpha_1) = \varepsilon_0^{q_2}$  for  $f_1$  and  $\varepsilon^2 = \varepsilon_0^2 + (1 - \varepsilon_0^2)q_2$  for  $f_2$ ;
- (iv) calculate the scattering angle  $\theta_{\text{Compt}}$  from formula (12);
- (v) test the rejection function: if  $g(\varepsilon) \geq q_3$  accept  $\varepsilon$ , otherwise go to step (i).

After the successful sampling of  $\varepsilon$  and the polar angles  $\theta_{\text{Compt}}$  of the scattered photon with respect to the direction of the parent photon, the kinetic energy and momentum of the recoil electron are then determined by

$$T_{e_{\text{recoil}}} = E_0 - E_1, \tag{16}$$

$$\mathbf{P}_{e_{\text{recoil}}} = \mathbf{P}_0 - \mathbf{P}_1, \tag{17}$$

$E_0$  and  $P_0$  are the energy and momentum of the parent photon;  $E_1$  and  $P_1$  are the energy and momentum of the scattered photon;  $T_{e_{\text{recoil}}}$  and  $P_{e_{\text{recoil}}}$  are the energy and momentum of the recoil electron.

c) For the gamma conversion into an  $(e^+, e^-)$  pair simulation for total energy carried by one particle of the pair is based on the Bethe–Heiler differential cross-section formula [9]:

$$\frac{d\sigma(Z, \varepsilon)}{d\varepsilon} = \alpha r_e^2 Z[Z + \xi(Z)] \left\{ [\varepsilon^2 + (1 - \varepsilon)^2] \left[ \Phi_1(\delta(\varepsilon)) - \frac{F(Z)}{2} \right] + \left[ \frac{2\varepsilon(1 - \varepsilon)}{3} \right] \left[ \Phi_2(\delta(\varepsilon)) - \frac{F(Z)}{2} \right] \right\}, \tag{18}$$

where  $\alpha$  is the fine-structure constant and  $r_e$  the classical electron radius;  $\varepsilon = E/E_0$ ,  $E_0$  is the energy of the photon and  $E$  is the total energy of one particle in the  $(e^+, e^-)$  pair. Therefore, the kinematical limit of  $\varepsilon$  is

$$\frac{m_e c^2}{E_0} \equiv \varepsilon_0 \leq \varepsilon \leq 1 - \varepsilon_0. \tag{19}$$

In cross-section formula (19) two screen functions  $\Phi_1(\delta)$  and  $\Phi_2(\delta)$  are introduced [9]:

(i) for  $\delta \leq 1$

$$\Phi_1(\delta) = 20.867 - 3.242\delta + 0.625\delta^2, \tag{20}$$

$$\Phi_2(\delta) = 20.209 - 1.930\delta - 0.086\delta^2;$$

(ii) for  $\delta > 1$

$$\Phi_1(\delta) = \Phi_2(\delta) = 21.12 - 4.184 \ln(\delta + 0.952), \tag{21}$$

where the screening variable  $\delta$  is a function of  $\varepsilon$ :

$$\delta(\varepsilon) = \frac{136\varepsilon_0}{Z^{1/3}\varepsilon(1-\varepsilon)}. \quad (22)$$

The Bethe–Heiler formula is established for plane waves. So, for Coulomb waves a correction, so-called a Coulomb correction function, should be introduced in

$$F(Z) = 8 \ln Z/3 \quad \text{for } E_0 < 50 \text{ MeV}, \quad (23)$$

$$F(Z) = 8 \ln Z/3 + 8f_c(Z) \quad \text{for } E_0 \geq 50 \text{ MeV}, \quad (24)$$

with

$$f_c(Z) = (\alpha Z)^2 \left\{ \frac{1}{1 + (\alpha Z)^2} + 0.20206 - 0.0369(\alpha Z)^2 + 0.0083(\alpha Z)^4 - 0.00020(\alpha Z)^6 + \dots \right\}. \quad (25)$$

The polar angle of the electron (or positron) is defined with respect to the direction of the parent photon. The energy-angle distribution can be approximated by a density function given by L. Urban [10]:

$$F(u) = \left[ \frac{9a^2}{9+d} \right] (u e^{-au} + du e^{-3au}) \quad (26)$$

with

$$a = 5/8, \quad d = 27 \text{ and } \theta_{\pm} = um_e c^2 / E_{\pm}. \quad (27)$$

A sampling of the distribution (27) requires a triplet  $(q_1, q_2, q_3)$  of random numbers such that

$$\text{if } q_1 < \frac{9}{9+d}, \text{ then } u = -\ln \frac{(q_2 q_3)}{a}, \text{ otherwise } u = -\ln \frac{(q_2 q_3)}{3a}. \quad (28)$$

In all calculations described above the azimuthal angle  $\psi$  is generated isotropically.

## 2. RESULTS AND DISCUSSION

Figure 1 shows calculations for the bremsstrahlung spectra produced by 18 MeV electron beams for cases of the thin W target (0.03 cm thick) and the thick one (0.3 cm thick), where the secondary interactions mentioned above were included in the simulation.

Figure 2 shows a dependence of emissions of secondary photons and electrons on the target thickness.

In these calculations the numbers of produced secondary particles, i.e., photons and electrons at the exit of target, were calibrated by one incident electron. This is to expose the role of secondary processes that occur in the target in the formation of the energy distribution of bremsstrahlung.

It can be seen from Figs.1 and 2 that due to the secondary interactions the numbers of electrons and photons emitted from the target could be increased, respectively, by up to factors of approximately 4 and 6 compared with that of incident electrons.

The simulation of the spectral characteristics as a function of the target thickness showed that this increase of the photons is mainly due to the sequent bremsstrahlung emissions from

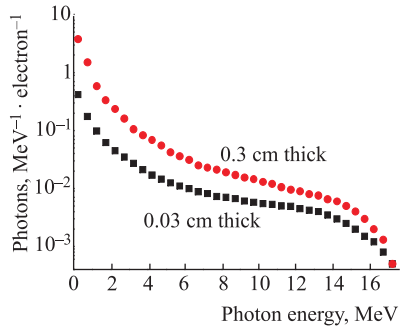


Fig. 1. Bremsstrahlung spectrum produced by 18 MeV electron beams on W targets

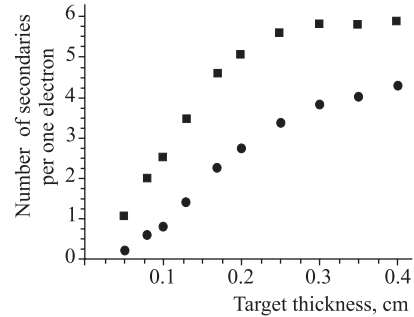


Fig. 2. Number of photons (■) and electrons (●) as a function of W-target thickness

the scattered electrons in the target. For a gross bremsstrahlung spectrum these photons make a broadening in the angular distributions. From the above-mentioned results for the dependence of the photon intensity on the target thickness we would like to show the two following comments:

1. For the nuclear reaction research with bremsstrahlung, the calculations in optimizing both the necessary photon intensity and the possible angular broadening as a function of the thickness should be taken into account.

2. From Fig. 1 we can see that enhance of the photons is mainly located at low energies, i.e., at those below the threshold of reactions  $(\gamma, p)$ ,  $(\gamma, np)$ ,  $(\gamma, xn)$  and  $(\gamma, xp)$  for the light nuclei. This suggests a possibility to use the bremsstrahlung emission from the thick target to produce high-intensity neutron sources by low-threshold  $(\gamma, n)$  reactions, for a typical example  ${}^9\text{Be}(\gamma, n){}^8\text{Be}$ .

## CONCLUSION

We have used the Monte-Carlo calculations to study the secondary interactions induced by the bremsstrahlung and the electrons produced by braking accelerated relativistic electron beams in thick target. Our calculations were performed on the basis of energy and angular distributions of the emitted particles. These distributions are parameterized either from experimental data or from theoretical description. This allowed us to consider contributions of the secondary effects to the production yields of bremsstrahlung and electrons emitted from the target. In this study the role of the secondary interaction effects was explicitly exposed by considering the emission of photons and electrons as a function of target thickness. For the bremsstrahlung emission from a thick target the simulation showed the increase of the photon intensity and the possible broadening in angular distributions in the region of photonuclear reactions due to the secondary electron emission. Therefore, the optimization calculations for target thickness based on a compromise between two these effects should be taken into account in photonuclear reaction research. Moreover, the simulation showed a possibility to produce the high-intensity neutron source by using low-threshold  $(\gamma, n)$  reactions from the bremsstrahlung emission in case of the thick target.

**Acknowledgements.** This work has been performed with the financial support by the National Research Program on Natural Science under grant No.403806. We would like to express sincere thanks for this precious assistance.

#### REFERENCES

1. *Findlay D. J.* // Nucl. Instr. Meth. A. 1989. V.276. P.598.
2. *Zhuchko V. E., Tsipenyuk Yu. M.* // Atomn. Energiya. 1975. V. 39. P.66 (in Russian).
3. *Khai N. T., Thiep T. D.* // Commun. Phys. 2003. V. 13, No. 3. P. 149.
4. *Marmier P., Sheldon E.* Physics of Nuclei and Particles. N. Y.; London: Acad. Press, 1969. V.1.
5. *Leo W. R.* Techniques for Nuclear and Particle Physics Experiments. Berlin; Heidelberg: Springer-Verlag, 1987; 1994.
6. *Wheeler J. A., Land W. E.* // Phys. Rev. 1939. V.55. P.858.
7. *Storm E., Israel H.* Photon Cross-Sections from 1 keV to 100 MeV for Elements  $Z = 1$  to  $Z = 100$ . Los Alamos Sci. Lab., Univ. of California, Los Alamos, New Mexico. 87544.
8. *Gavrila M.* // Phys. Rev. 1959. V. 113. P.514.
9. *Heiler W.* The Quantum Theory of Radiation. Oxford Univ. Press, 1957.
10. *Urban L.* GEANT3 Writeup. Section PHYS-211. CERN Program Library, 1993.

Received on May 16, 2007.